TAIWANESE JOURNAL OF MATHEMATICS
Vol. 18, No. 6, pp. 1739-1757, December 2014
DOI: 10.11650/tjm.18.2014.4092
This paper is available online at http://journal.taiwanmathsoc.org.tw

TESTING IMPROVEMENTS OF A WELL-BALANCED METHOD FOR THE MODEL OF A FLUID IN A NOZZLE WITH VARIABLE CROSS-SECTION

Mai Duc Thanh and Dietmar Kröner

Abstract. A set of improvements of a well-balanced scheme for the model of fluid flows in a nozzle with variable cross-section is presented. Relying on the well-balanced method introduced in our earlier work, we use the steady state solutions to absorb the nonconservative term. The underlying numerical fluxes operating on these steady states are obtained as convex combinations of the numerical fluxes of a first-order and a second-order schemes. The improvements are still well-balanced schemes. Then, we present many numerical tests, which establishes the efficiency of these numerical schemes. These schemes can provide us with very desirable approximations for any initial data: data in supersonic or subsonic regions, and data in both of these two kinds of regions. All the tests also show that the accuracy of the method by the improvements is improved.

1. Introduction

In this paper we are concerned with improvements of the accuracy and the robustness of the well-balanced numerical method proposed earlier in [20] for the following model of fluid flows in a nozzle with variable cross-section

$$\begin{aligned} &\partial_t(a\rho) + \partial_x(a\rho u) \;=\; 0,\\ &\partial_t(a\rho u) + \partial_x(a(\rho u^2 + p)) \;=\; p\partial_x a,\\ &\partial_t(a\rho e) + \partial_x(au(\rho e + p)) = 0, \quad x \in \boldsymbol{R},\, t > 0, \end{aligned} \tag{1.1}$$

where $a = a(x), x \in \boldsymbol{R}$ represents the cross-section, ρ is the density, u is the velocity, $e = \varepsilon + u^2/2$ is the total energy, ε is the internal energy, and p is the pressure. Usually, one supplements the system (1.1) with the trivial equation

$$\partial_t a = 0, \tag{1.2}$$

Received November 24, 2013, accepted March 13, 2014.
Communicated by Wen-Wei Lin.
2010 *Mathematics Subject Classification*: 35L65, 65M06, 76T10.
Key words and phrases: Well-balanced scheme, Fluid dynamics, Discontinuous nozzle, Accuracy, Efficiency, Source term.

when investigating the properties of the system, see [22].

In [20], we have proposed a well-balanced scheme, relying on the Lax-Friedrichs scheme and the treatment of the source term of (1.1). This scheme has been shown to work well when data are either in supersonic or subsonic regions. Recently, in [33], we introduced some computing correctors, which help the scheme in [20] to overpass difficulties in approximating solutions across the sonic surface. In this work, we will consider to improve the accuracy and the robustness of the method. Motivated by a recent work [35] for an isentropic model of two-phase flows, we take the underlying numerical flux to be convex combinations of the ones of the first-order Lax-Friedrichs scheme - which can assure the convergence to the entropy solutions, but rather diffusive- and of the second-order Richtmyer scheme. Observe that second-order schemes may not converge to the entropy solutions. Moreover, the family is equipped with the computing corrector proposed in our earlier work [33]. This computing corrector is aimed at making sure that the method can work well for data across the sonic surface (the exact solutions are located in both subsonic and supersonic regions). We then provide many tests of these schemes for various kinds of initial data to verify the robustness and therefore the efficiency of the schemes. These improvements are still well-balanced schemes, i.e., that they can capture exactly steady state solutions. Furthermore, certain choices of the parameter yield well-balanced schemes which can attain an accuracy much faster. The accuracy of this kind of schemes at the same mesh size is much better than the scheme using only underlying numerical flux of the Lax-Friedrichs scheme. Finally, tests also indicate that convex combinations of a low-order scheme and a high-order numerical scheme need not to improve the order of convergence of the lower scheme.

Many works concerning the model (1.1) can be found in the literature. The study of hyperbolic systems of balance laws in nonconservative form has been carried out in [10, 26, 23, 30, 17, 14, 2, 24]. Numerical approximations for the model (1.1) were considered in [20, 19, 28, 18]. Numerical approximations for the related model of shallow water equations with discontinuous topography were studied in [7,18, 13, 25]. Recently, a numerical treatment for shallow water equations with variable topography is proposed in [34]. Several well-balanced numerical schemes for a single conservation law with source term were studied in [16, 5, 6, 15, 3]. Numerical schemes for multi-phase flows and other models were studied in [4, 21, 29, 1, 31, 32, 35, 36]. Numerical schemes for nonconservative hyperbolic systems were considered in [27, 8, 11, 12, 9]. See also the references therein.

The organization of this paper is as follows. In Section 2 we recall basic concepts and properties of the model (1.1). Section 3 is devoted to the construction of the family of the well-balanced schemes. The computing correctors are also given. In Section 4, we present numerical tests to verify the robustness, the well-balanced property, and finding the accuracy of the method. Finally, in Section 5 we provide conclusions and discussions.

2. Preliminaries

For simplicity, throughout we assume that the fluid is polytropic and ideal:

$$p = (\gamma - 1)\,\rho\varepsilon,$$

such that the equation of state can be given in the form

$$p = p(\rho, S) = (\gamma - 1)\exp\left(\frac{S - S_*}{C_v}\right)\rho^\gamma,$$

where S is the specific entropy, $\gamma > 1$ is the adiabatic exponent, $C_v > 0$ is the specific heat at constant volume, and S_* is constant. Observe that for a polytropic and ideal fluid, γ and C_v are constants.

The system (1.1)-(1.2) can be written in the vector form

$$U_t + A(U)U_x = 0, \tag{2.1}$$

where $U = (\rho, u, S, a)$, and

$$A(U) = \begin{pmatrix} u & \rho & 0 & \frac{u\rho}{a} \\ \frac{p_\rho}{\rho} & u & \frac{p_S}{\rho} & 0 \\ 0 & 0 & u & 0 \\ 0 & 0 & 0 & 0 \end{pmatrix}. \tag{2.2}$$

The matrix $A(U)$ in (2.2) admits four real eigenvalues,

$$\lambda_0 = 0, \quad \lambda_1 = u - c, \quad \lambda_2 = u, \quad \lambda_3 = u + c, \tag{2.3}$$

where c is the *local sound speed*

$$c = \sqrt{p_\rho} = \sqrt{\gamma p(\rho, S)/\rho}.$$

Since the characteristic field associated with λ_0 may coincide with any other field, the system (2.1) is *not strictly hyperbolic*. Set

$$\begin{aligned} &G_1 = \{U : \lambda_0(U) < \lambda_1(U) < \lambda_2(U) < \lambda_3(U)\}, \\ &G_2 = \{U : \lambda_1(U) < \lambda_0(U) < \lambda_2(U) < \lambda_3(U)\}, \\ &G_3 = \{U : \lambda_1(U) < \lambda_2(U) < \lambda_0(U) < \lambda_3(U)\}, \\ &G_4 = \{U : \lambda_1(U) < \lambda_2(U) < \lambda_3(U) < \lambda_0(U)\}. \\ &\Sigma_+ = \{U : \lambda_1(U) = \lambda_0(U)\}, \\ &\Sigma_0 = \{U : \lambda_2(U) = \lambda_0(U)\}, \\ &\Sigma_- = \{U : \lambda_3(U) = \lambda_0(U)\}, \\ &\Sigma = \Sigma_+ \cup \Sigma_- \cup \Sigma_0. \end{aligned} \tag{2.4}$$

The *supersonic region* is the one in which

$$|u| > c,$$

which corresponds to $G_1 \cup G_4$. The *subsonic region* is the one in which

$$|u| < c,$$

which corresponds to $G_2 \cup G_3$. The *sonic surface* is the one on which

$$|u| = c,$$

which corresponds to $\Sigma_\pm$.

As shown in [30], a right-hand state $U_1 = (\rho_1, u_1, S_1, a_1)$ can be connected with a left-hand state $U_0 = (\rho_0, u_0, S_0, a_0)$ via a stationary wave if

$$\begin{aligned} &[a\rho u] = 0, \\ &\Big[\frac{u^2}{2} + h(\rho, S_0)\Big] = 0, \\ &[S] = 0, \end{aligned} \tag{2.5}$$

where $[S] = S_1 - S_0$, etc, and h is the specific enthalpy given by

$$h(\rho, S) = p + \varepsilon/\rho = \gamma \exp\Big(\frac{S - S_*}{C_v}\Big)\rho^{\gamma-1}. \tag{2.6}$$

Set

$$A(S) = (\gamma - 1)\exp\Big(\frac{S - S_*}{C_v}\Big), \quad \kappa = A(S_0), \quad \mu = \frac{2\kappa\gamma}{\gamma - 1}. \tag{2.7}$$

The density satisfies

$$F(U_0, a; \rho) := \mu\rho^\gamma - \Big(u_0^2 + \mu\rho_0^{\gamma-1}\Big)\rho + \Big(\frac{a_0 u_0 \rho_0}{a}\Big)^2 \frac{1}{\rho} = 0, \quad \rho > 0, \tag{2.8}$$

where μ is defined by (2.7). Set

$$\begin{aligned} q_1 &= \frac{a_0 u_0 \rho_0}{a\sqrt{u_0^2 + \mu\rho_0^{\gamma-1}}}, \\ q_2 &= \left(\frac{u_0^2}{\mu} + \rho_0^{\gamma-1}\right)^{1/(\gamma-1)}. \end{aligned} \tag{2.9}$$

It has been known that the nonlinear algebraic equation (2.8) may possess two real roots, which give two possible density values. These yields two possible stationary contacts for each given left-hand state and a level of cross-section of the right-hand state. However, from a state in the subsonic or supersonic region, there is only one admissible stationary contact wave, which corresponds to a sole admissible density value. In [33], it is shown that the admissible density value will be computed by the Newton-Raphson method for (2.8) starting at q_1 if U_0 is in the supersonic region, and at q_2 if U_0 is in the subsonic region.

3. Improving the Accuracy of Well-balanced Schemes

3.1. Combining with high-order schemes

When $a =$ constant, the system (1.1) can be reduced to the usual gas dynamics equations

$$\partial_t V + \partial_x f(V) = 0, \tag{3.1}$$

where

$$V = \begin{pmatrix} \rho \\ \rho u \\ \rho e \end{pmatrix}, \quad f_1(V) := \begin{pmatrix} \rho u \\ \rho u^2 + p \\ u(\rho e + p) \end{pmatrix}.$$

Set

$$x_j = j\Delta x, j \in \mathbf{Z}, \quad t_n = n\Delta t, n \in \mathbf{N}, \quad \lambda = \frac{\Delta t}{\Delta x}.$$

The following C.F.L. stability condition is required

$$CFL = \lambda \cdot \max_U \{|\lambda_i(U)|, i = 1, 2, 3\} < 1. \tag{3.2}$$

Explicit schemes for (3.1) are given by

$$U_j^{n+1} = U_j^n - \lambda(g(U_{j+1}^n, U_j^n) - g(U_j^n, U_{j-1}^n)), \quad j \in \mathbf{Z}, n \in \mathbf{N}, \tag{3.3}$$

where $g(U, V)$ is the numerical flux.

The numerical flux of the Lax-Friedrichs scheme is given by

$$g_{LF}(U, V) = \frac{1}{2}\big(f(U) + f(V)\big) - \frac{1}{2\lambda}(V - U). \tag{3.4}$$

The numerical flux of Richtmyer's scheme, which is a second-order scheme, is given by

$$g_R(U, V) = f\left(\frac{U + V}{2} - \frac{\lambda}{2}(f(V) - f(U))\right). \tag{3.5}$$

Convex combinations of these two numerical fluxes

$$g_\theta(U, V) := (1 - \theta)g_{LF}(U, V) + \theta g_R(U, V), \quad 0 \le \theta \le 1, \tag{3.6}$$

define a one-parameter set of numerical schemes for (3.1). In the next section we will be involved with the two special choices of θ:

$$\theta_1 = \frac{1}{1 + CFL}, \quad \theta_2 = 0.9.$$

Let $g_\theta = g_\theta(U, V)$ be an *underlying* numerical flux of the family (3.6). Our well-balanced scheme for (1.1) is defined by

$$U_j^{n+1} = U_j^n - \lambda\big(g_\theta(U_j^n, U_{j+1,-}^n) - g_\theta(U_{j-1,+}^n, U_j^n)\big). \tag{3.7}$$

In the scheme (3.7), the states

$$U_{j+1,-}^n = (\rho, \rho u, \rho e)_{j+1,-}^n, \quad U_{j-1,+}^n = (\rho, \rho u, \rho e)_{j-1,+}^n$$

are defined as follows. First, observe that the entropy is constant across each stationary jump, we compute $\rho_{j+1,-}^n, u_{j+1,-}^n$ from the equations

$$\begin{aligned} &a_{j+1}^n \rho_{j+1}^n u_{j+1}^n = a_j^n \rho_{j+1,-}^n u_{j+1,-}^n, \\ &\frac{(u_{j+1}^n)^2}{2} + h(\rho_{j+1}^n) = \frac{(u_{j+1,-}^n)^2}{2} + h(\rho_{j+1,-}^n), \end{aligned} \tag{3.8}$$

and we compute $\rho_{j-1,+}^n, u_{j-1,+}^n$ from the equations

$$\begin{aligned} &a_{j-1}^n \rho_{j-1}^n u_{j-1}^n = a_j^n \rho_{j-1,+}^n u_{j-1,+}^n, \\ &\frac{(u_{j-1}^n)^2}{2} + h(\rho_{j-1}^n) = \frac{(u_{j-1,+}^n)^2}{2} + h(\rho_{j-1,+}^n). \end{aligned} \tag{3.9}$$

It is not difficult to verify that the schemes (3.7) are well-balanced. That is, they can maintain the stationary contacts of the system (1.1). Indeed, if the initial data $U_0(x)$ correspond to a stationary contact, then it holds that

$$\begin{aligned} &a_{j+1}^n \rho_{j+1}^n u_{j+1}^n = a_j^n \rho_j^n u_j^n, \\ &\frac{(u_{j+1}^n)^2}{2} + h(\rho_{j+1}^n) = \frac{(u_j^n)^2}{2} + h(\rho_j^n), \end{aligned}$$

for $j \in \mathbf{Z}, n = 0, 1, 2, \ldots$. The last two equations yield

$$\begin{aligned} &\rho_{j+1,-}^n = \rho_j^n, \quad u_{j+1,-}^n = u_j^n, \\ &\rho_{j-1,+}^n = \rho_j^n, \quad u_{j-1,+}^n = u_j^n, \end{aligned}$$

for $j \in \mathbf{Z}, n = 0, 1, 2, \ldots$. Thus,

$$U_{j+1,-}^n = U_j^n, \quad U_{j-1,+}^n = U_j^n,$$

and so it is derived from (3.7) that

$$U_j^{n+1} = U_j^n, \qquad j \in \mathbf{Z}, n = 0, 1, 2, ..,$$

i.e., the schemes can capture exactly the stationary contact wave.

3.2. Completing the method by equipping with computing correctors

Existing schemes often fail to approximate solutions when data belong to both sides of the sonic surface $\Sigma_{\pm}$. In particular, a scheme may not work when a rarefaction wave is attached by a stationary wave that jumps into the other side of the sonic surface. This has been observed in [33], where a numerical treatment to overcome this obstacle is proposed by introducing a suitable computing corrector such that the algorithm selecting the admissible stationary contact wave in the construction of the well-balanced scheme works properly. The computing correctors make sure that the errors do not influence the choice of the admissible density of the nonlinear equation (2.8) when the numerical data are very closed to the sonic surface. In particular, when the rarefaction wave approaches the sonic surface and the solution tends to come across the sonic boundary, the computing corrector is designed to make the scheme take the stationary wave that helps the solution to overcome this sonic surface. Furthermore, to be consistent, the computing correctors are required to be as a modulus of continuity of Δx. Precisely, the two computing correctors are defined as follows.

(I) A mesh-size dependent corrector:

$$d_j^n = \Delta x \max_{i=1,2,3} |\lambda_i(U_j^n)| \left(|\rho_{j+1}^n - \rho_j^n| + |u_{j+1}^n - u_j^n| + |p_{j+1}^n - p_j^n|\right), \tag{3.10}$$

(II) Corrector depends on the number of the iterations:

$$d_j^n = \frac{\max_{i=1,2,3} |\lambda_i(U_j^n)|}{\sqrt{k}} \left(|\rho_{j+1}^n - \rho_j^n| + |u_{j+1}^n - u_j^n| + |p_{j+1}^n - p_j^n|\right), \tag{3.11}$$

where k is the number of iterations.

The correctors work in the following way: *if* $(u_j^n)^2 - p_\rho(\rho_j^n, S_j^n) < -d_j^n$ *(instead of* $(u_j^n)^2 - p_\rho(\rho_j^n, S_j^n) \leq 0$*), then starting the Newton-Raphson method at* q_1 *defined by (2.9) for solving the nonlinear equation (2.8) to get* $\rho_{j,\pm}^n$*. Otherwise, starting the Newton-Raphson method at* q_2 *defined by (2.9) for solving (2.8) to get* $\rho_{j,\pm}^n$*.* This is because when studying the Riemann problem for (1.1) (see [30]), we realize that only rarefaction waves approach the sonic surface from the subsonic region in a Riemann solution and the solution attains the sonic surface before continuing across this sonic surface from the subsonic region to the supersonic region. Thus, the correctors can help the solution come across the sonic surface. Without such a corrector, the solution may approach the sonic surface and then come back into the subsonic domain by a possibly large stationary wave, yielding a possibly big error.

In the next section we will investigate to see whether the family of well-balanced schemes with the underlying numerical fluxes (3.6) equipped with one of the computing correctors (3.11) can deal with data around the sonic surface.

4. Test Cases

In this section we will provide several tests with the family of numerical schemes (3.7) with the two special choices $\theta_1 = 1/(1+CFL)$ and $\theta_2 = 0.9$. The scheme (3.7) with the underlying numerical flux given by (3.6 with $\theta = 1/(1+CFL)$ will be referred to as the *FAST1* scheme, while $\theta = 0.9$ corresponds to the *FAST2* scheme. The scheme (3.7) with the underlying numerical flux given by (3.6) with the trial choice $\theta = 0$ will be referred to as the *Lax-Friedrichs-type* (LF-type for short) scheme. These schemes are then equipped with the first computing corrector in (3.11) with the hope that they will work for any initial data (robustness). The test 1 is devoted to a stationary wave, and the other three tests are devoted to observations of the robustness, the accuracy, and the CPU times of the schemes. Let the parameters are chosen to be

$$\gamma = 1.4, \quad C_v = 1, \quad S_* = 1.$$

Consider the Riemann problem for (1.1)-(1.2) with the Riemann data

$$U_0(x) = \begin{cases} U_L = (\rho_L, u_L, p_L, a_L), & x < 0, \\ U_R = (\rho_R, u_R, p_R, a_R), & x > 0. \end{cases} \tag{4.1}$$

4.1. Test 1: Steady state solutions

This test is devoted to a steady state solution (stationary wave). We consider the Riemann problem for (1.1)-(1.2), where the initial data (4.1) are given by Table 1.

Table 1. The initial data of the Riemann problem for (1.1)-(1.2) for Test 1

$\diagdown$	ρ	u	p	a
U_L	3	5	5	1
U_R	1.9284239	5.1855819	2.6932939	1.5

It is not difficult to check that this Riemann data correspond to the left-hand and right-hand states of a steady state solution, which is a stationary contact wave.

The approximate solution is computed on the interval $[-1, 1]$ with 500 mesh points at the time $t = 0.1$ using the scheme (3.6) with $\theta = 0.9$, called the *FAST2 scheme*. The approximate solution is plotted in Figure 1, which shows that the scheme captures exactly the steady state solution. This means that the scheme (3.6) is *well-balanced.*

4.2. Test 2: Solution in subsonic region

In this test, the Riemann solution lies entirely in the subsonic region. The Riemann data are taken in the subsonic region, i.e., $U_L, U_R \in G_2$. The exact Riemann solution is taken from [30]. The solution is a 1-shock from U_L to U_1, followed by a stationary

wave from U_1 to U_2, a 2-contact discontinuity from U_2 to U_3, and finally from U_3 to U_R by a 3-rarefaction wave. The states U_L, U_R, U_1, U_2, U_3 are given in Table 2.

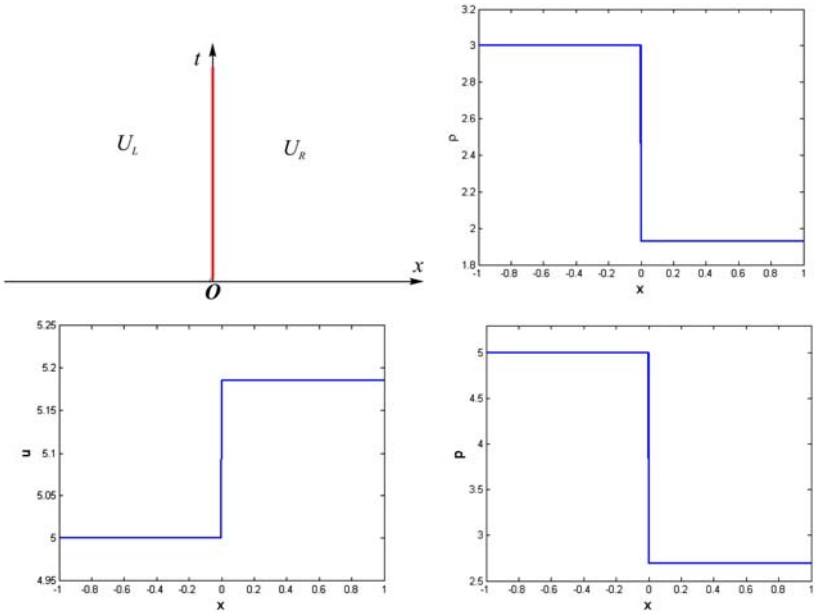

Fig. 1. Test 1: Approximation of a stationary contact wave by FAST2 scheme at the time t = 0:1 with 500 mesh points on the interval $[-1; 1]$.

Table 2. States that separate the elementary waves of the exact Riemann solution in Test 2, see Figure 2 (upper-left corner)

	ρ	u	p	a
U_L	1.3939394	1.9325048	6	1
U_1	2	1	10	1
U_2	2.048658	0.81354072	10.342255	1.2
U_3	1.048658	0.81354072	10.342255	1.2
U_R	1.40092	1.9214873	15.513383	1.2

The approximate solution will be computed at the time $t = 0.1$ on the interval $[-1, 1]$ of the x-space using the underlying numerical fluxes of the Lax-Friedrischs scheme, FAST1 and FAST2 schemes with different mesh sizes. Figure 2 shows the plots of the approximate solutions given by the Lax-Friedrichs-type scheme, the FAST1 and the FAST2 scheme with the mesh-size $h = 1/250$. Figure 3 displays the approximate solutions by the FAST2 scheme with different mesh sizes $h = 1/125, 1/500, 1/2000$. These figures show good approximations of the exact solution. The approximate solution given by the FAST2 scheme is the finest one. The errors in the L^1 norm are computed and the orders of convergence are estimated, and are reported by Table 3.

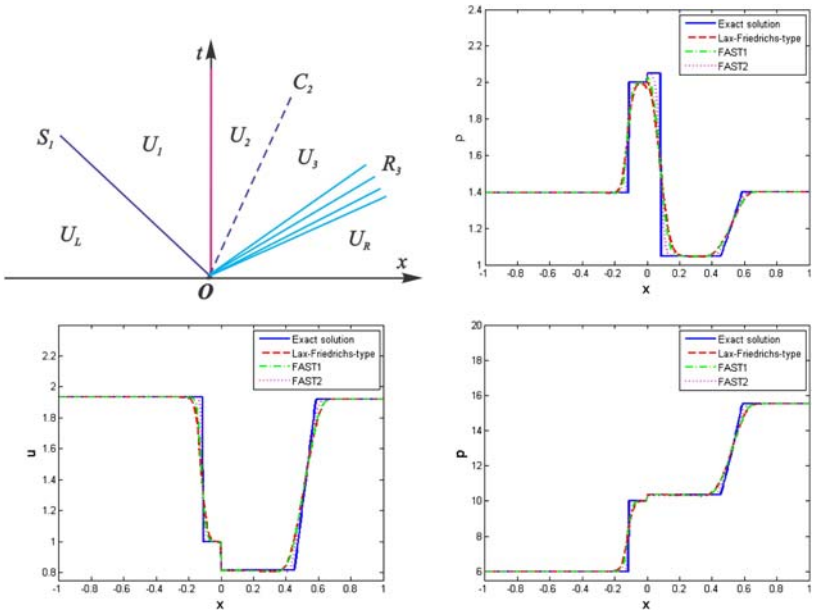

Fig. 2. Test 2: Approximate solution by the Lax-Friedrichs-type, FAST1, and FAST2 schemes with 500 mesh points on the interval $[-1; 1]$.

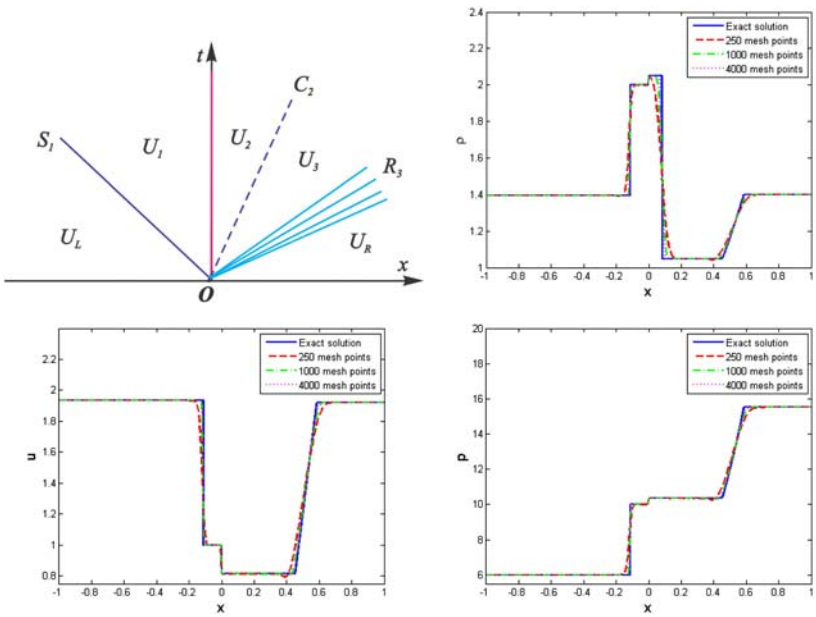

Fig. 3. Test 2: Approximate solution using the underlying FAST2 numerical ux. The approximate solution is computed at the time $t = 0.1$ on the interval $[-1; 1]$ with 250, 1000, and 4000 mesh points, and is compared with the exact solution.

Table 3 indicates that at the same mesh-sizes, the FAST1 scheme gives a better accuracy than the Lax-Friedrichs-type scheme, and the FAST2 scheme gives a better than the FAST1 scheme. At the same mesh-sizes, the Lax-Friedrichs-type scheme is the fastest. The iteration numbers are almost the same. However, the most important observation here is that to get the same (or approximate) accuracy, the Lax-Friedrichs-type scheme and the FAST1 scheme require much more time than the FAST2 scheme.

Table 3. Test 2: Errors, orders of convergence, numbers of iterations, and CPU times of the well-balanced schemes

LF-type

N	L^1-Error	Order	Iterations	CPU time
250	0.47301	–	147	7.1604
500	0.30887	0.61	293	17.145
1000	0.1894	0.71	586	56.644
2000	0.11395	0.73	1172	212.6
4000	0.067159	0.76	2344	1087.6

FAST1

N	Error	Order	Iterations	CPU time
250	0.40292	–	147	11.232
500	0.25933	0.64	293	33.275
1000	0.15655	0.73	586	110.75
2000	0.093914	0.74	1172	437.47
4000	0.055678	0.75	2344	2057.4

FAST2

N	Error	Order	Iterations	CPU time
250	0.19026	–	147	10.967
500	0.11667	0.71	293	32.682
1000	0.065239	0.84	586	110.01
2000	0.038942	0.74	1172	433.21
4000	0.023447	0.73	2344	2015.8

4.3. Test 3: Solution in supersonic region

In this test, the Riemann solution lies entirely in the supersonic region. The Riemann data are taken in the subsonic region: $U_L, U_R \in G_1$. The exact Riemann solution is taken from [30]. The exact Riemann solution begins with a stationary contact wave from U_L to U_1, followed by a 1-shock from U_1 to U_2, a 2-contact discontinuity from U_2 to U_3, and finally from U_3 to U_R by a 3-shock wave. The states U_L, U_R, U_1, U_2, U_3 are given in Table 4.

Table 4. Test 3: States that separate the elementary waves of the exact Riemann solution, see Figure 4 (upper-left corner)

$\diagdown$	ρ	u	p	a
U_L	1	6	3	1.5
U_1	1.5995235	5.6266756	5.7903943	1
U_2	2.5992257	4.4467026	11.580789	1
U_3	3.5992257	4.4467026	11.580789	1
U_R	2.2149081	3.4439598	5.7903943	1

The approximate solution will be computed at the time $t = 0.1$ on the interval $[-1, 1]$ of the x-space using the underlying numerical fluxes of the Lax-Friedrischs scheme, FAST1 and FAST2 schemes with different mesh sizes. Figure 4 shows the plots of the approximate solutions given by the Lax-Friedrichs-type scheme, the FAST1 and the FAST2 scheme with the mesh-size $h = 1/250$. Figure 5 displays the approximate solutions by the FAST2 scheme with different mesh sizes $h = 1/125, 1/500, 1/2000$. These figures show good approximations of the exact solution. The approximate solution given by the FAST2 scheme is the finest one. The errors in the L^1 norm are computed and the orders of convergence are estimated, and are reported by Table 5.

Table 5 indicates that at the same mesh-sizes, the FAST1 scheme gives a better

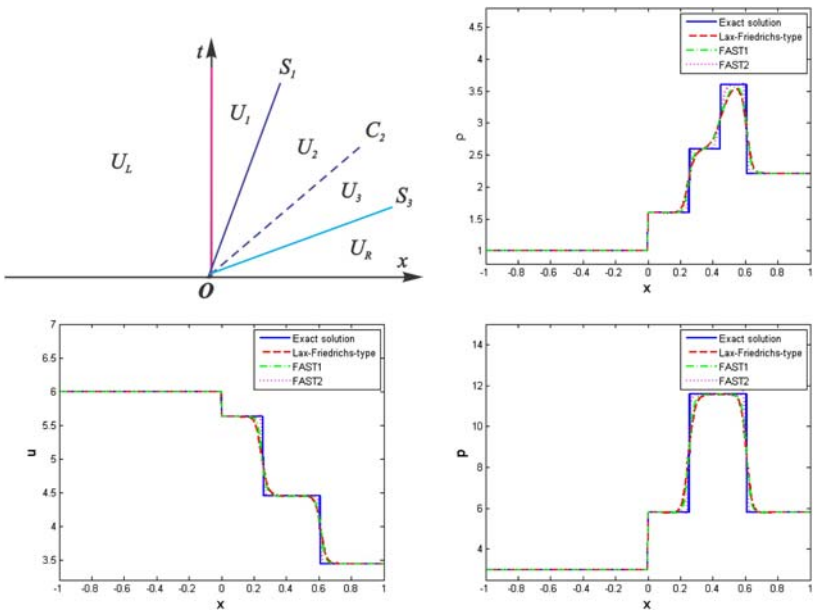

Fig. 4. Test 3: Approximate solution by the Lax-Friedrichs-type, FAST1, and FAST2 schemes with 500 mesh points on the interval $[-1; 1]$.

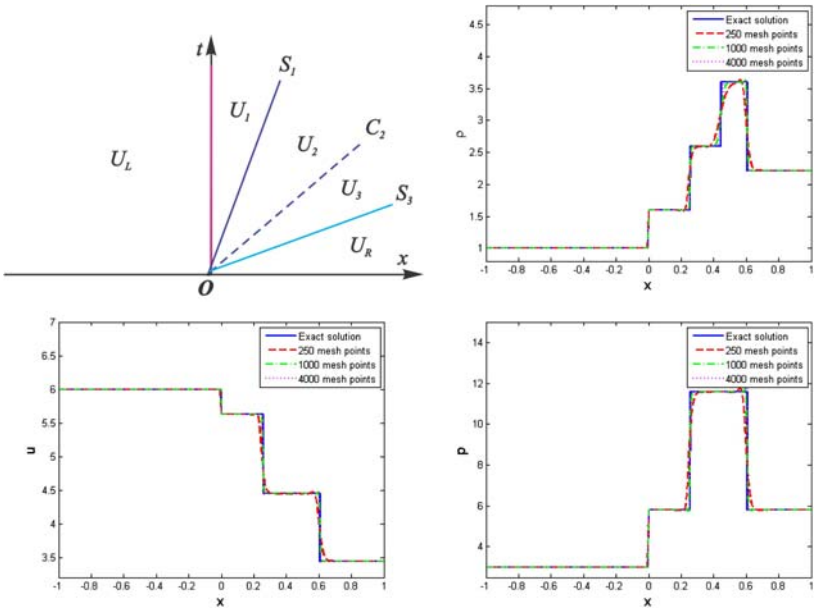

Fig. 5. Test 3: Approximate solution using the underlying FAST2 numerical ux. The approximate solution is computed at the time $t = 0 : 1$ on the interval $[-1; 1]$ with 250, 1000, and 4000 mesh points, and is compared with the exact solution.

accuracy than the Lax-Friedrichs-type scheme, and the FAST2 scheme gives a better than the FAST1 scheme. The orders of convergence are almost the same. At the same mesh-sizes, the Lax-Friedrichs-type scheme is the fastest. The iteration numbers are almost the same. Interestingly, the FAST2 scheme is the fastest one attaining the same (or approximate) accuracy.

4.4. Test 4: Solution in resonant regime

In this test, the Riemann data are taken on the opposite sides of the resonance surface, where $U_L \in G_2$ and $U_R \in G_1$.

The solution begins with a 1-rarefaction wave from U_L in the subsonic region G_2 to U_1 on the sonic surface, followed by a stationary wave from U_1 to U_2 in the supersonic region G_1, then followed by a 2-contact discontinuity from U_2 to U_3, and finally followed from U_4 to U_R by a 3-shock wave. The states U_L, U_R, U_1, U_2, U_3 are given in Table 6.

The approximate solution will be computed at the time $t = 0.2$ on the interval $[-1, 1]$ of the x-space using the underlying numerical fluxes of the Lax-Friedrichs scheme, FAST1 and FAST2 schemes with different mesh sizes. Figure 6 shows the plots of the approximate solutions given by the Lax-Friedrichs-type scheme, the FAST1 and the FAST2 scheme with the mesh-size $h = 1/250$. Figure 7 displays the approximate solutions by the FAST2 scheme with different mesh sizes $h = 1/125, 1/500, 1/2000$.

These figures show good approximations of the exact solution. The approximate solution given by the FAST2 scheme is the finest one. The errors in the L^1 norm are computed and the orders of convergence are estimated, and are reported by Table 7.

Table 5. Test 3: Errors, orders of convergence, numbers of iterations, and CPU times of the well-balanced schemes

LF-type

N	L^1-Error	Order	Iterations	CPU time
250	0.71061	–	202	9.9685
500	0.43966	0.69	403	25.085
1000	0.25523	0.78	805	74.366
2000	0.13907	0.88	1610	321.44
4000	0.074094	0.91	3220	1458.6

FAST1

N	Error	Order	Iterations	CPU time
250	0.57938	–	202	15.382
500	0.34797	0.74	403	45.459
1000	0.19652	0.82	805	151.93
2000	0.10534	0.9	1610	603.83
4000	0.056288	0.9	3220	2627.3

FAST2

N	Error	Order	Iterations	CPU time
250	0.24168	–	202	15.428
500	0.1378	0.81	403	44.632
1000	0.07011	0.97	806	154.99
2000	0.03904	0.84	1611	596.58
4000	0.021274	0.88	3221	2628.5

Table 6. Test 4: States that separate the elementary waves of the exact Riemann solution, see Figure 6 (upper-left corner)

$\diagdown$	ρ	u	p	a
U_L	5	0.5	8	1
U_1	2.7766	1.3306	3.5111	1
U_2	1.6697	1.8438	1.7227	1.2
U_3	2.0779	1.5738	2.3427	1.2
U_4	1.8047	1.5738	2.3427	1.2
U_R	1	0.8	1	1.2

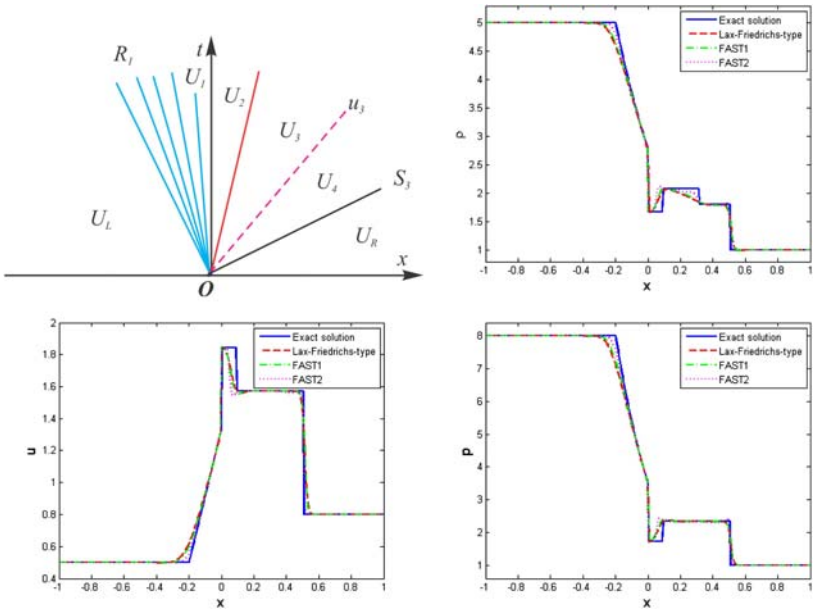

Fig. 6. Test 4: Approximate solution by the Lax-Friedrichs-type, FAST1, and FAST2 schemes with 500 mesh points on the interval $[-1; 1]$ at the time $t = 0.2$.

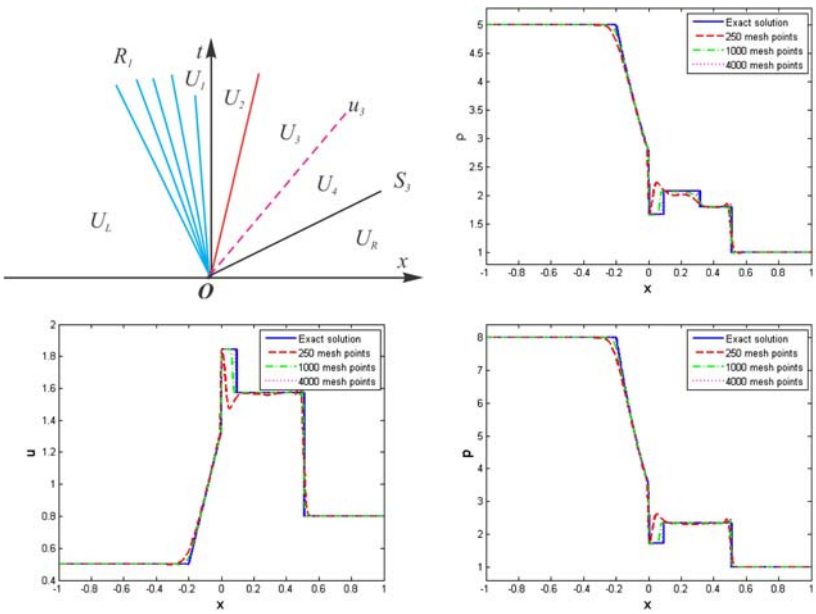

Fig. 7. Test 4: Approximate solution using the underlying FAST2 numerical ux. The approximate solution is computed at the time $t = 0.2$ on the interval $[-1; 1]$ with 250, 1000, and 4000 mesh points, and is compared with the exact solution.

Table 7 indicates that at the same mesh-sizes, the FAST1 scheme gives a better accuracy than the Lax-Friedrichs-type scheme, and the FAST2 scheme gives a better than the FAST1 scheme. At the same mesh-sizes, the Lax-Friedrichs-type scheme is the fastest. The orders of convergence are increasing from Lax-Friedrichs-type scheme to FAST1 and FAST2 schemes. The iteration numbers are almost the same. However, the most important observation here is that to get the same (or approximate) accuracy, the Lax-Friedrichs-type scheme and the FAST1 scheme require much more time than the FAST2 scheme.

Table 7. Test 4: Errors, orders of convergence, numbers of iterations, and CPU times of the well-balanced schemes

LF-type

N	L^1-Error	Order	Iterations	CPU time
250	0.4302	–	148	10.967
500	0.24649	0.8	300	25.397
1000	0.14285	0.79	605	71.386
2000	0.084304	0.76	1214	254.13
4000	0.04944	0.77	2433	1151.7

FAST1

N	Error	Order	Iterations	CPU time
250	0.38408	–	148	14.726
500	0.21337	0.85	300	40.654
1000	0.11945	0.84	605	129.89
2000	0.068624	0.8	1214	483.38
4000	0.039285	0.8	2432	2237.9

FAST2

N	Error	Order	Iterations	CPU time
250	0.28346	–	149	14.773
500	0.14749	0.94	302	44.273
1000	0.074821	0.98	606	131.56
2000	0.041751	0.84	1216	480.81
4000	0.022374	0.9	2434	2086.1

5. Conclusions and Discussions

This work provides many tests for several remarkable improvements of the well-balanced schemes (3.7) for the model of a fluid in anozzle with variable cross-section (1.1). The complete description of the improvements can be described as follows.

First, we deal with the nonconservative term on the right-hand side of (1.1) using stationary wave, which was done in [20]. This step could absorb the nonconservative term. Second, we consider the improvement of the accuracy by forming the underlying numerical fluxes of (3.7) to be convex combinations of the numerical fluxes of the first-order Lax-Friedrichs scheme and the second-order Richtmyer scheme as in (3.6). Finally, these schemes are equipped with the computing correctors (3.11), which were proposed in [33], in such a way that it can work for data across the sonic surface from the subsonic region to the supersonic region.

The schemes in this family are shown to be well-balanced, that is, they can capture exactly steady state solutions. Tests show that after equipping the computing corrector proposed in [33], the schemes in this family can work for any initial data in supersonic or subsonic regions, or both even initial data in both supersonic and subsonic regions. So, the robustness of the method can be confirmed. Moreover, this construction of family of schemes can produce fast schemes, where the accuracy can be attained within a much shorter time than the sole application of the Lax-Friedrichs scheme as originally proposed in [20]. The accuracy of the scheme obtained from this family by certain choices of the parameter θ such as $\theta = 0.9$ can give much better accuracy than the scheme using only the first-order Lax-Friedrichs scheme. We also observe from the tests that convex combinations of numerical fluxes of the first-order Lax-Friedrichs scheme and the second-order Ritchmyer's scheme might not yield higher orders of convergence.

References

1. A. Ambroso, C. Chalons, F. Coquel and T. Galié, Relaxation and numerical approximation of a two-fluid two-pressure diphasic model, *ESAIM: M2AN*, **43** (2009), 1063-1097.
2. N. Andrianov and G. Warnecke, On the solution to the Riemann problem for the compressible duct flow, *SIAM J. Appl. Math.*, **64** (2004), 878-901.
3. E. Audusse, F. Bouchut, M.-O. Bristeau, R. Klein and B. Perthame, A fast and stable well-balanced scheme with hydrostatic reconstruction for shallow water flows, *SIAM J. Sci. Comput.*, **25** (2004), 2050-2065.
4. F. Bouchut, *Nonlinear Stability of Finite Volume Methods for Hyperbolic Conservation Laws, and Well-balanced Schemes for Sources*, Frontiers in Mathematics Series, Birkhäuser, 2004.
5. R. Botchorishvili, B. Perthame and A. Vasseur, Equilibrium schemes for scalar conservation laws with stiff sources, *Math. Comput.*, **72** (2003), 131-157.
6. R. Botchorishvili and O. Pironneau, Finite volume schemes with equilibrium type discretization of source terms for scalar conservation laws, *J. Comput. Phys.*, **187** (2003), 391-427.
7. A. Chinnayya, A.-Y. LeRoux and N. Seguin, A well-balanced numerical scheme for the approximation of the shallow water equations with topography: the resonance phenomenon, *Int. J. Finite Vol.*, **1(4)** (2004).

8. M. J. Castro, J. M. Gallardo and C. Parés, High-order finite volume schemes based on reconstruction of states for solving hyperbolic systems with nonconservative products. Applications to shallow-water systems, *Math. Comput.*, **75** (2006), 1103-1134.
9. M. J. Castro, P. G. LeFloch, M. L. Muñoz-Ruiz and C. Parés, Why many theories of shock waves are necessary: convergence error in formally path-consistent schemes, *J. Comput. Phys.*, **227** (2008), 8107-8129.
10. G. Dal Maso, P. G. LeFloch and F. Murat, Definition and weak stability of nonconservative products, *J. Math. Pures Appl.*, **74** (1995), 483-548.
11. M. Dumbser, M. Castro, C. Pars and E. F. Toro, ADER schemes on unstructured meshes for nonconservative hyperbolic systems: applications to geophysical flows, *Computers & Fluids*, **38** (2009), 1731-1748.
12. M. Dumbser, A. Hidalgo, M. Castro, C. Pars and E. F. Toro, FORCE schemes on unstructured meshes II: non-conservative hyperbolic systems, *Computer Methods in Applied Mechanics and Engineering*, **199** (2010), 625-647.
13. T. Gallouët, J.-M. Hérard and N. Seguin, Numerical modeling of two-phase flows using the two-fluid two-pressure approach, *Math. Models Methods Appl. Sci.*, **14** (2004), 663-700.
14. P. Goatin and P. G. LeFloch, The Riemann problem for a class of resonant nonlinear systems of balance laws, *Ann. Inst. H. Poincar Anal. NonLinéaire*, **21** (2004), 881-902.
15. L. Gosse, A well-balanced flux-vector splitting scheme designed for hyperbolic systems of conservation laws with source terms, *Comput. Math. Appl.*, **39** (2000), 135-159.
16. J. M. Greenberg, A. Y. Leroux, R. Baraille and A. Noussair, Analysis and approximation of conservation laws with source terms, *SIAM J. Numer. Anal.*, **34** (1997), 1980-2007.
17. E. Isaacson and B. Temple, Convergence of the 2×2 Godunov method for a general resonant nonlinear balance law, *SIAM J. Appl. Math.*, **55** (1995), 625-640.
18. S. Jin and X. Wen, Two interface type numerical methods for computing hyperbolic systems with gometrical source terms having concentrations, *SIAM J. Sci. Comput.*, **26** (2005), 2079-2101.
19. D. Kröner, P. G. LeFloch and M. D. Thanh, The minimum entropy principle for fluid flows in a nozzle with discntinuous crosssection, *ESAIM: M2AN*, **42** (2008), 425-442.
20. D. Kröner and M. D. Thanh, Numerical solutions to compressible flows in a nozzle with variable cross-section, *SIAM J. Numer. Anal.*, **43** (2005), 796-824.
21. M.-H. Lallemand and R. Saurel, Pressure relaxation procedures for multiphase compressible flows, *INRIA Report, No. 4038*, 2000.
22. P. G. LeFloch, Shock waves for nonlinear hyperbolic systems in nonconservative form, *Institute for Math. and Its Appl., Minneapolis, Preprint*, #593, 1989.
23. P. G. LeFloch and M. D. Thanh, The Riemann problem for fluid flows in a nozzle with discontinuous cross-section, *Comm. Math. Sci.*, **1** (2003), 763-797.
24. P. G. LeFloch and M. D. Thanh, The Riemann problem for shallow water equations with discontinuous topography, *Comm. Math. Sci.*, **5** (2007), 865-885.
25. P. G. LeFloch and M. D. Thanh, A Godunov-type method for the shallow water equations with variable topography in the resonant regime, *J. Comput. Phys.*, **230** (2011), 7631-7660.

26. D. Marchesin and P. J. Paes-Leme, A Riemann problem in gas dynamics with bifurcation. Hyperbolic partial differential equations III, *Comput. Math. Appl. (Part A)*, **12** (1986), 433-455.
27. C. Parés, Numerical methods for nonconservative hyperbolic systems: a theoretical framework, *SIAM J. Numer. Anal.*, **44** (2006), 300-321.
28. D. Rochette, S. Clain and W. Bussire, Unsteady compressible flow in ducts with varying cross-section: comparison between the nonconservative Euler system and the axisymmetric flow model, *Computers & Fluids*, **53** (2012), 53-78.
29. R. Saurel and R. Abgrall, A multi-phase Godunov method for compressible multifluid and multiphase flows, *J. Comput. Phys.*, **150** (1999), 425-467.
30. M. D. Thanh, The Riemann problem for a non-isentropic fluid in a nozzle with discontinuous cross-sectional area, *SIAM J. Appl. Math.*, **69** (2009), 1501-1519.
31. M. D. Thanh, D. Kröner and C. Chalons, A robust numerical method for approximating solutions of a model of two-phase flows and its properties, *Appl. Math. Comput.*, **219** (2012), 320-344.
32. M. D. Thanh, D. Kröner and N. T. Nam, Numerical approximation for a Baer-Nunziato model of two-phase flows, *Appl. Numer. Math.*, **61** (2011), 702-721.
33. M. D. Thanh and D. Kröner, Numerical treatment of nonconservative terms in resonant regime for fluid flows in a nozzle with variable cross-section, *Computers & Fluids*, **66** (2012), 130-139.
34. M. D. Thanh and M. D. Thanh, Numerical treatment in resonant regime for shallow water equations with discontinuous topography, *Commun. Nonl. Sci. Num. Simulat.*, **18** (2013), 417-433.
35. M. D. Thanh, Building fast well-balanced two-stage numerical schemes for a model of two-phase flows, *Commun. Nonlinear Sci. Numer. Simulat.*, **19** (2014), 1836-1858.
36. M. D. Thanh, Well-balanced Roe-type numerical scheme for a model of two-phase compressible flows, *Kor. J. Math.*, **51(1)** (2014), 163-187.

Mai Duc Thanh
Department of Mathematics
International University
Quarter 6, Linh Trung Ward
Thu Duc District, Ho Chi Minh City
Vietnam
E-mail: mdthanh@hcmiu.edu.vn

Dietmar Kröner
Institute of Applied Mathematics
University of Freiburg
Hermann-Herder Str. 10
79104 Freiburg
Germany
E-mail: dietmar@mathematik.uni-freiburg.de